

Nanococoon seeds for BN nanotube growth

M. V. P. ALTOE, J. P. SPRUNCK, J.-C. P. GABRIEL, K. BRADLEY*
Nanomix Inc., 5980 Horton Street, Suite 600, Emeryville, CA 94608, USA
E-mail: kbradley@nano.com

A modification in the conventional arc-discharge method for synthesis of nanotubes is presented. By injecting pure nitrogen gas directly into the plasma we have greatly increased the amount of boron nitride nanotubes produced. Isolated nanotubes and bundles were characterized by TEM. The vast majority of the nanotubes were double-walled with outer diameter around 3 nm. The predominance of double-walled BN nanotubes is seen as a direct result of the distribution of the number of graphitic BN layers for the nanococoons, second major product of the synthesis. Detailed HRTEM examination of the ends of BN nanotubes indicates continuity between the graphitic BN layers that coat boron nanoparticles, that is nanococoon, and the nanotube. At the other end of the nanotubes a flat angular cap was observed. HRTEM images of nanotube ends give support to a root-based growth mechanism. © 2003 Kluwer Academic Publishers

1. Introduction

Based upon similarities between carbon and boron nitride, BN nanotubes were first theoretically proposed [1] and then synthesized [2–9] using routes similar to that used for carbon nanotubes, i.e., arc-discharge, laser ablation and CVD. BN nanotubes are attractive because of their unique electronic, thermal and mechanical properties. Unlike carbon nanotubes, BN nanotubes are semiconductors with a wide band gap that is weakly dependent on the helicity and diameter of the tubes [10]. In comparison with single wall carbon nanotubes (SWCNTs), relatively little is known about the growth of boron nitride nanotubes (BNNTs). For example, in carbon nanotubes it is well established that growth includes solvation of carbon into metal clusters and precipitation of excess carbon in the form of nanotubes. Such a mechanism has not yet been demonstrated for BNNTs. Indeed, BN nanotubes were prepared without using catalyst in a laser ablation route with nanotube growth originated from a pure boron nanoparticle [7].

The growth mechanisms for SWCNTs have been separated into tip-growth and root-growth types. In tip growth, carbon atoms diffuse along the tube stem to the open tip [11–13]. Single metal atoms chemisorbed onto the open edge would have a crucial role on this type of growth, both assisting in the formation of carbon hexagons and inhibiting the formation of pentagons that would initiate dome closure [14, 15]. In root growth, a nanotube extends from atoms added to its base [16]. By imaging the ends of nanotubes with TEM, one can glean their growth mechanism. In fact, TEM imaging of both ends of isolate SWCNTs has provided a clear evidence for the root-growth model [17, 18], that is, the catalyst nanoparticle remains stationary, whereas a nanotube grows out from the particle with a closed-end.

TEM images have unambiguously showed individual SWCNTs with one end containing a catalyst nanoparticle and the other end closed, ruling out the tip growth model at least for the case of growth of SWCNTs from discrete catalytic nanoparticles [17, 18].

For BNNTs, both types of model remain strong candidates. TEM imaging of both ends of one BNNT is very rare specially for the case of nanotubes synthesized in a arc-plasma method due to the relatively long length of the nanotubes (in the μ range) added to the fact that the ends are very often buried in the nanoparticle clusters co-generated in the discharge. Tip-growth mechanism is weakly supported by a report of metal compounds on the tip of BNNTs [2] and observation of one open-ended BNNT [6]. However, most BNNTs ends reported in the literature are closed. In the case of BNNT prepared without catalyst [7] observation of ends with encapsulated boron nanoparticles are interpreted as evidence that BNNT grow via a root-based mechanism. B nanoparticles at the root are thought to react with N_2 to form BNNTs.

We explored BNNT synthesis by arc discharge. A modified arc chamber was built to optimize the yield of BNNTs. The product material was investigated using SEM and TEM. Particular attention was paid to the nanotube ends, in an attempt to elucidate the mechanism of BNNT growth.

2. Experimental section

Conductive boron electrodes were prepared by skull-melting elemental boron (crystalline ingot, Alpha Aesar 99.5%) with 1% nickel and 1% cobalt in a 17 psia argon atmosphere in a commercial arc furnace. After several refinement melts, homogeneous 5 g boron ingots were obtained with resistivities below 5 ohm-cm. Boron

*Author to whom all correspondence should be addressed.

ingots were attached to water-cooled copper electrodes using mechanical clamps.

The electrodes were mounted perpendicular to each other. The side electrode was manipulated by a linear motion controller, and the bottom electrode was tilted manually to establish an arc. At voltages of 40 V, dc currents of about 30 A were maintained for periods of about 20 s. After this time, the boron ingots were observed to melt; they were allowed to cool for 20 s between arcs.

Pure nitrogen gas was introduced to the chamber through two distinct lines. One line supplied nitrogen to the main chamber through a water-cooled arm. Several arms were available on the chamber; best results were obtained using the arm perpendicular to the plane of the electrodes. A second line added nitrogen directly to the plasma through a 1/8" stainless steel tube. Optimal production was found with the tube positioned 1" from the ingots. Nitrogen was removed continuously through a pumping port directly above the plasma; material was filtered from the gas stream by a copper mesh.

The flow of nitrogen through the steel tube was controlled between 5 and 20 Lpm. Chamber pressure, nitrogen flow rate, and arc current were varied to optimize nanotube production. Abundance of nanotubes was obtained using pressures between 200 Torr and 450 Torr, nitrogen flow near 15 Lpm, and currents of 30 A. The arc generated an unstable plume 1–2" in diameter. Fine, long strands of black material streamed upwards from the plume. After arcing, a gray web-like material was recovered from the copper mesh, and gray soot was found on the walls and bottom of the chamber.

Two types of purification were attempted. To remove residual metal and unreacted boron, the material was boiled in nitric acid. Although this process preferentially removed boron from boron nitride cocoons [6], it also removed boron nitride nanotubes. No nanotubes were observed after nitric acid treatments. A separation by density was therefore employed to remove large particles. Material was sonicated for dispersal in a mixture

of bromoform and 1,1,1-trichloroethane in such ratio that its density was intermediate between boron nitride and boron. Since boron is denser than boron nitride, after centrifugation at 14,000 rpm, purified BN material was drawn from the top of the suspensions.

Samples of material were sonicated in 1,2-dichlorobenzene, dispersed on a silicon wafer surface and gold coated for characterization by SEM (Leo 1530, 5 kV). TEM analysis was performed in samples dispersed onto holey carbon film 300 mesh copper grid. Analytical work was conducted in a JEOL JEM 200CX TEM at 100 KV equipped with a Gatan 666 parallel collection Electron Energy Loss Spectrometer (PEELS). High Resolution TEM (HRTEM) images were obtained in a 002B-TOPCON microscope at 120 KV.

3. Results and discussion

The web-like material collected from the copper mesh was considerably richer in nanotubes than the soot from the walls and bottom of the chamber. Fig. 1 shows a typical SEM image of a web sample as collected. The material consisted of nanotubes tens of microns in length, connected by nanoparticles. Larger particles up to microns in diameter were also observed. These particles were removed by centrifugation.

TEM images of the web structures show isolated nanotubes or small bundles, as shown in Fig. 2a. Electron energy loss spectra (EELS) confirmed that the nanotubes and bundles exhibited characteristic boron and nitrogen K edges. Detailed examinations were made to compare BN nanotube (BNNT) bundles and typical single-walled carbon nanotube (SWCNT) bundles. Several significant differences could be observed. First, SWCNT bundles often originate from single particles. By contrast, the BNNT bundles extended between adjacent areas rich in nanoparticle clusters, and nanotubes within each bundle appeared to originate from different clusters. Second, SWCNT bundles typically comprise uniform nanotubes arranged in parallel to form

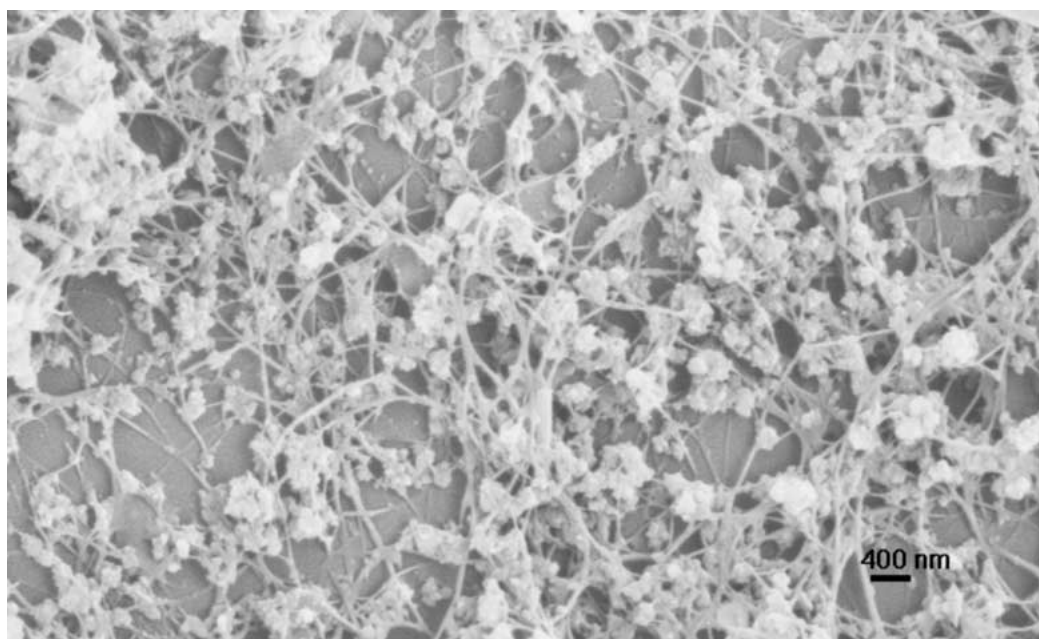


Figure 1 SEM image of web like material. BN nanotubes can easily reach several microns in length and are systematically associated with nanoparticles.

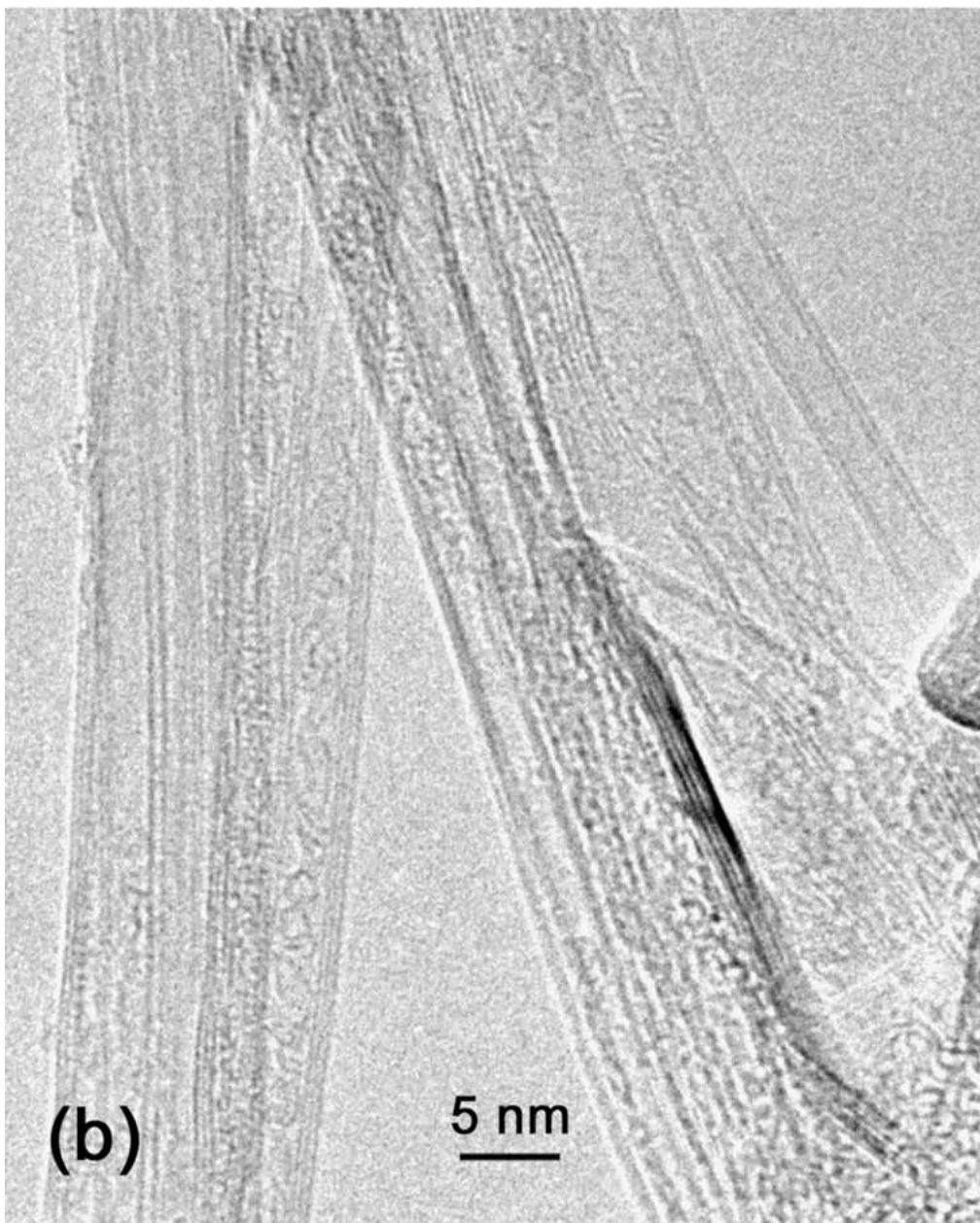
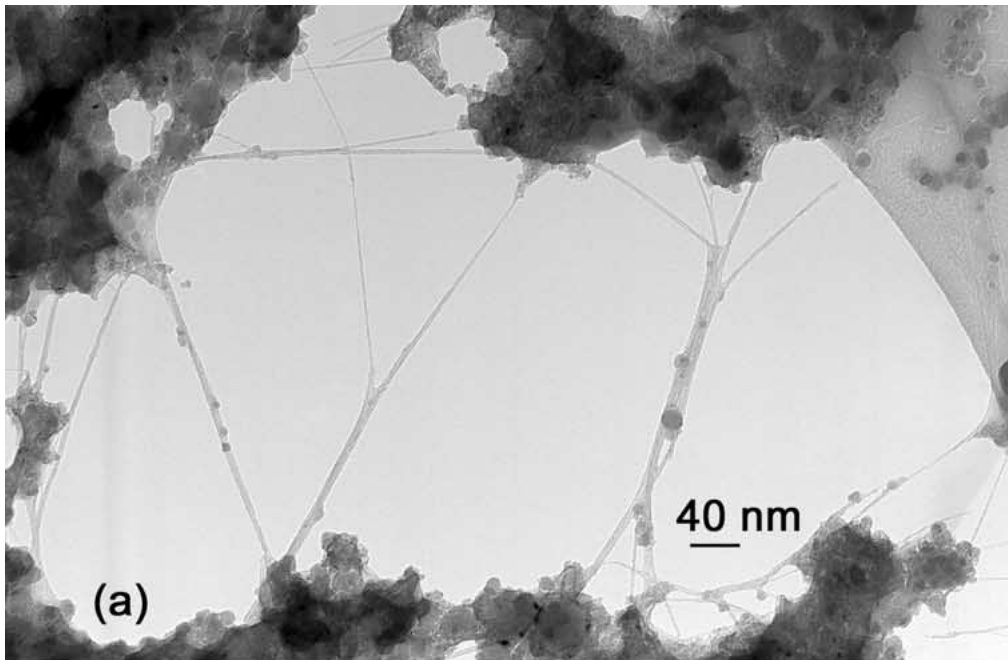


Figure 2 (a) TEM image of BN nanotubes extending between adjacent areas rich in nanoparticle and (b) HRTEM of BN nanotube bundle.

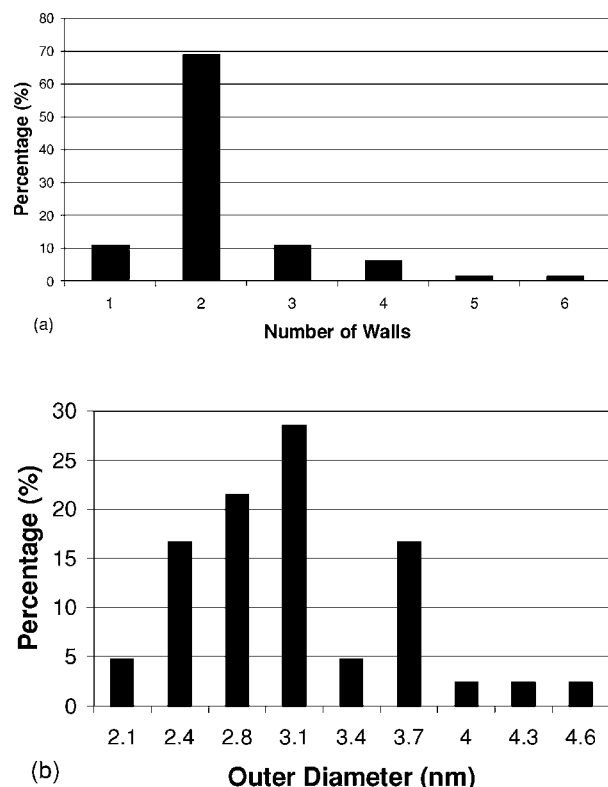


Figure 3 (a) Histogram of number of walls in BN nanotubes observed in web-like material. Double wall BN nanotube predominance is remarkable. A total of 64 nanotubes were analyzed and (b) Histogram of outer diameters, in nm, of double wall BN nanotube observed in web-like material. A total of 42 DWBNNT were measured

lattices. Fig. 2b shows that the BNNTs were nonuniform in diameter and in number of walls. In addition, individual nanotubes were not parallel within bundles. They separated from bundles and rejoined the bundles at various points along their lengths. Third, SWCNTs usually have open interiors. Most BNNTs were similarly empty. However, some double-walled and triple-walled BNNTs featured peapod structures in their interiors. These may be boron nitride analogues of icosahedral fullerenes [19, 20]. Finally, several closed ends of BNNTs were observed, as shown in Fig. 5d. These ends were blunt, right-angled caps, as opposed to the rounded caps common in SWCNTs. This characteristic angular BN cap has been attributed to the presence of squares, rather than pentagons, as the most common defect [21]. No open-ended BNNTs were found.

Samples from multiple runs were imaged by HRTEM to quantify the number of walls and the diameters of BNNTs. The distribution of number of walls in BN nanotubes for a total of 64 nanotubes, shown in Fig. 3a, shows a pronounced majority of double-walled nanotubes. Similar distribution was reported by Cumings and Zettl [6] for BNNTs produced by arc discharge. However, we additionally observed a significant fraction of nanotubes with odd numbers of walls. In particular, 10% of the nanotubes were single-walled. We also measured the distribution of outer diameters of double-walled BN nanotubes, shown in Fig. 3b. Most of the 42 nanotubes measured had outer diameters between 2.4 and 3.7 nm. This distribution is wider than has been reported for SWCNTs in bundles [15] and double-wall BN nanotubes [6]. Wide distributions have been suggested to cause randomness in bundle arrangements in some SWCNT growth [10].

A striking observation was that all attempts using several types of solvents and sonication times employed to separate nanoparticles and nanotubes failed. The nitric acid boiling procedure was successful in removing metal and unreacted boron but also eliminated all nanotubes. This result stimulated more detailed TEM work to examine the connection between nanotubes and nanoparticles.

First, the nanoparticles themselves were characterized. HRTEM images together with EELS and electron diffraction data revealed that those nanoparticles associated with BN nanotubes were B rich nanocrystals coated with a few layers of graphitic BN, boron filled nanococoons, terminology introduced in reference [6]. Some of those nanoparticles also contained cobalt and nickel impurities. The BN nanococoons showed a wide range of sizes from 5 to 100 nm. The number of BN layers of the nanococoon did not show any clear correlation with its diameter. As an example, in Fig. 4 one can see boron particles that are about the same size but coated with different numbers of graphitic BN layers. However, in general only a small number of layers of graphitic BN were observed. Interestingly, very frequently the nanococoons consist of two layers of BN. The BN nanococoon did not make intimate contact with the boron nanocrystals over their entire surfaces. Instead, the layers exhibited sharp facets and nanocrystals had rounded corners. Distinct gaps were apparent in such places, as can be seen in Fig. 5a.

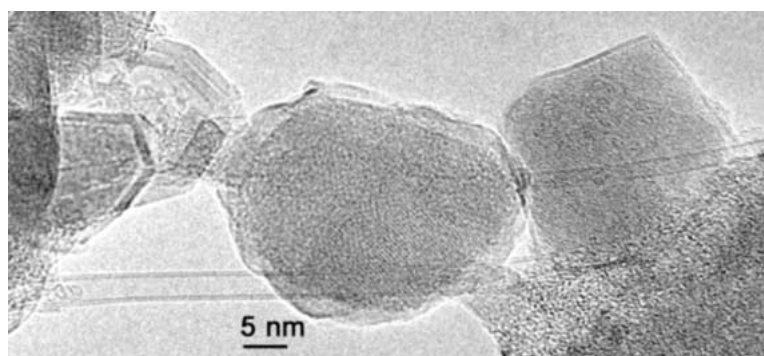


Figure 4 HR-TEM of web-like material as collected from the arc-chamber. Double-wall BN nanotubes and B-rich nanoparticles coated with graphitic BN layers, BN nanococoons, were major constituents of the sample. Also, one single wall BN nanotube is shown.

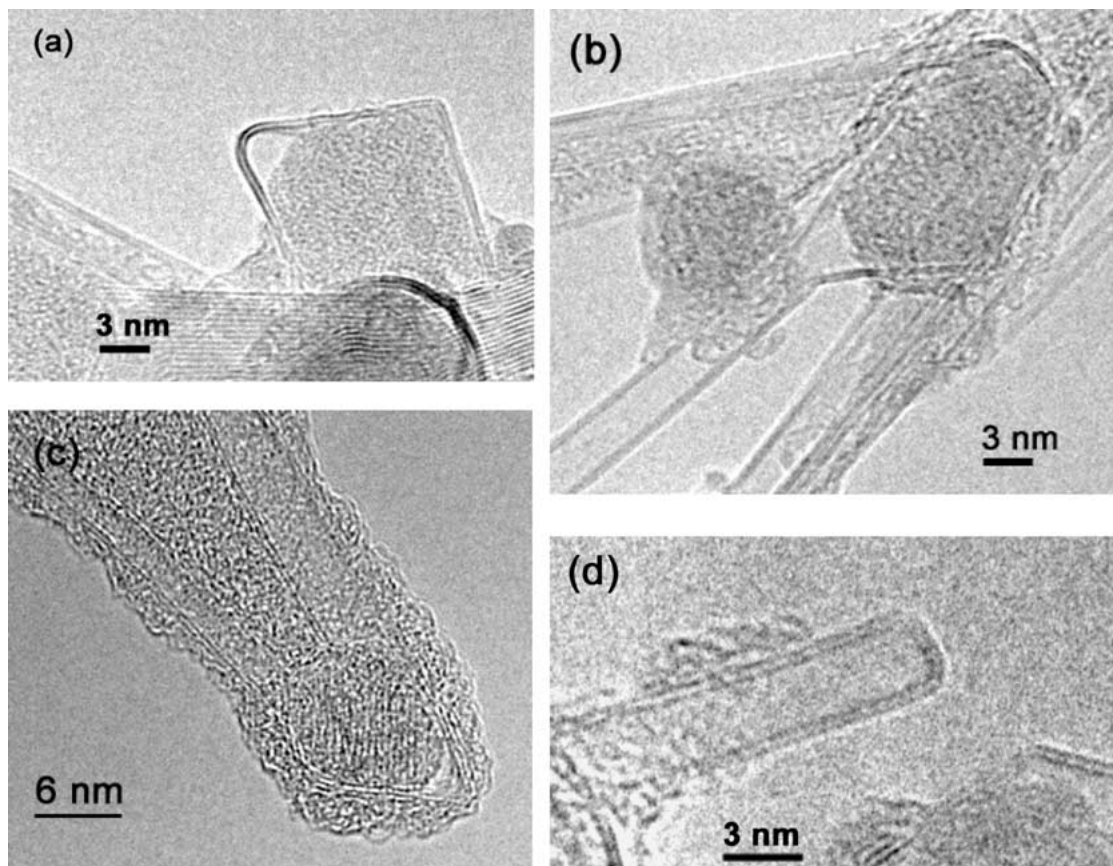


Figure 5 HRTEM images: (a) sharp facets of a double layer of graphitic BN coating a boron particle. The coating layers do not wet completely the boron particle surface suggesting that the formation of the coating is posterior to the boron particle formation, (b) a double-wall BN nanotube with a double layer nanococoon end, (c) two double-wall nanotubes with a common nanococoon end, and (d) a flat angular cap end.

Second, the contact between nanococoons and nanotubes was investigated. Two types of contact were observed. Both types are visible in Fig. 5b and c. In the first type, nanococoons were found on the side walls of nanotubes. The nanococoons were clearly distinct from the nanotubes, and presumably these nanococoons were attached by Van der Waals' forces. The second type of contact took place at the end of nanotubes. In these contacts, the BN sheets were continuous between the nanococoons and the nanotubes. The nanotube-nanococoon junctions took place at the corners, rather than within facets.

We interpret these observations in terms of the mechanism of BN nanotube growth. The growth mechanism is distinctly different from that of carbon nanotubes. One difference is the role of the transition metals. In carbon nanotube growth, these metals form the nanoparticles from which nanotubes grow. They are therefore regarded as catalysts. As Lee *et al.* [7] have pointed out, the transition metals are not associated with the growth of BN nanotubes. In our samples, no transition metals were detected in any particle from which a nanotube grew. Hence the transition metals may simply serve as dopants to enhance the conductivity of the boron ingots.

A second, more striking difference is the role of the nanoparticles as a seed in the root growth mechanism. In both SWCNTs and BNNTs, nanotubes grow by the addition of atoms to the nanoparticles. As more material is added, closed-end nanotubes extend from the catalyst particles. For SWCNTs, carbon atoms are be-

lieved to dissolve in the transition metal particles. Carbon atoms then precipitate in the form of nanotubes. By contrast, the BN nanotubes are clearly connected to the BN nanococoons.

We propose the following scenario for the growth of BNNTs in arc discharge. Our scenario is similar to the suggestion that was made by Maiti *et al.* [16] for the growth of CNTs. The plasma contains droplets of molten boron from the ingots, boron vapor, and nitrogen vapor. The droplets have various sizes, and the larger droplets fall to the bottom of the chamber. The smallest droplets, nanometers in diameter, remain in the plasma. During their exposure to the plasma, boron and nitrogen atoms react on their surface to form boron nitride sheets. The formation of these sheets must take place after the droplets have solidified. Otherwise, the boron cores would completely fill the nanoparticles, in contrast to our observations. Those gaps between BN sheets and boron particle could not be explained by boron contraction because hexagonal BN has higher coefficient of thermal expansion than boron. The sheets have one or more layers; we have observed that two layers is the most common configuration. These sheets continue to grow in extent, remaining flat. At the junction of two or more flat sheets, defects are necessary to introduce curvature [16]. These defects are loci of nanotube growth. As boron and nitrogen atoms continue to be added to the sheets, they are incorporated into growing nanotubes at the tube base. Nanotube growth ends when the particle is transported out of the zone of hot gas.

This interpretation is supported by the observations. In particular, we have imaged a clear continuity between nanotubes and the layers of the nanococoons. In addition, we have inferred that boron nanoparticles are solid during nanotube growth. Boron and nitrogen atoms are much more likely to add to the coating of solid particles than to dissolve into the bulk. Besides, if nanotubes had grown directly from the solid particles, there should be nanotubes rooted in the side walls of some nanoparticles. On the contrary, we have found nanotubes growing only from the junctions of boron nitride facets. Furthermore, the association of one nanotube to one facet causes nanotubes to grow in many different directions from each nanoparticle, as in Fig. 5c. The disordered, unparallel bundling of the nanotubes is a result of this unparallel growth.

The growth scenario we have proposed clarifies our understanding of the BNNT wall number distribution. This distribution can now be seen to result directly from the distribution of layers of the nanococoons. For example, nanotubes are predominantly double-walled because the nanococoons are predominantly double-walled. The nanococoon wall distribution is probably a result of the permeability of boron and nitrogen through boron nitride. Consequently, the nanotube wall distribution can be explained in terms of basic physical properties of bulk boron nitride.

4. Conclusions

In conclusion, we have used a modified arc discharge chamber to synthesize a soot which is rich in boron nitride nanotubes. Odd-walled nanotubes were observed, including single-walled nanotubes. However, the majority of the nanotubes were double-walled. Detailed examination of the ends of the nanotubes indicates that all nanotubes grow from nanococoons. We have argued that growth takes place by a two-step process. First, boron nanoparticles act as seeds for strained boron nitride layers. Second, addition of boron and nitrogen to the layers produces nanotubes. This scenario explains why nanotubes are predominantly double-walled. This improved understanding of BNNT growth is important both for tailoring BNNT synthesis and for designing novel nanotube syntheses.

Acknowledgments

The authors thank the National Center of Electron Microscopy at Lawrence Berkeley National Laboratory for making the facility available to this work. This work was partially supported by the Director, Office of Science, Office of Basic Energy Sciences, of the U.S. Department of Energy under Contract No. DE-

AC03-76SF00098. We thank C. Echer for the assistance with AEM, A. Davis for the assistance with SEM, P. G. Collins for the assistance with equipment, S.H. Jhi for helpful discussion and S. P. Carol for critical reading the manuscript.

References

1. A. RUBIO, J. L. CORKILL and M. L. COHEN, *Phys. Rev. B* **49** (1994) 5081.
2. N. G. CHOPRA, R. J. LUYKEN, K. CHERREY, V. H. CRESPI, M. COHEN, S. G. LOUIE and A. ZETTL, *Science* **269** (1995) 966.
3. Z. WENG-SIEH, K. CHERREY, N. G. CHOPRA, X. BLASE, Y. MIYAMATO, A. RUBIO, M. L. COHEN, S. G. LOUIE and A. ZETTL, *Phys. Rev. B* **51** (1995) 11229.
4. A. LOISEAU, F. WILLAIME, N. DEMONCY, G. HUG and H. PASCARD, *Phys. Rev. Lett.* **76** (1996) 4737.
5. N. G. CHOPRA and A. ZETTL, *Solid State Commun.* **105** (1995) 297.
6. J. CUMINGS and A. ZETTL, *Chem. Phys. Lett.* **316** (2000) 211.
7. R. S. LEE, J. GAVILLET, M. LAMY DE LA CHAPPELLE, A. LOISEAU, J.-L. COCHON, D. PIGACHE, J. THIBAULT and F. WILLAIME, *Phys. Rev. B* **64** (2001) 121405-R.
8. D. GOLDBERG, Y. BANDO, L. BOURGEOIS, K. KURASHIMA and T. SATO, *Appl. Phys. Lett.* **77** (2000) 13.
9. R. MA, Y. BANDO and T. SATO, *Adv. Mater.* **14** (2002) 366.
10. X. BLASE, A. RUBIO, S. G. LOUIE and M. L. COHEN, *Europhys. Lett.* **28** (1994) 335.
11. S. IJIMA and T. ICHIHASHI, *Nature* **363** (1993) 603.
12. S. IJIMA, P. M. AJAYAN and T. ICHIHASHI, *Phys. Rev. Lett.* **69** (1992) 3100.
13. P. M. AJAYAN, J. M. LAMBERT, P. BERNIER, L. BARBEDETTE, C. COLLIEUX and J. M. PLANEIX, *Chem. Phys. Lett.* **215** (1993) 509.
14. Y. H. LEE, S. G. KIM and D. TOMANEK, *Phys. Rev. Lett.* **78** (1997) 2393.
15. A. THESS, R. LEE, P. NIKOLAEV, H. DAI, P. PETIT, J. ROBERT, C. XU, Y. H. LEE, S. G. KIM, A. G. RINZLER, D. T. COLBERT, G. E. SCUSERIA, D. TOMANEK, J. E. FISHER and E. SMALLEY, *Science* **273** (1996) 483.
16. A. MAITI, C. J. BRABEC and J. BERNHOLC, *Phys. Rev. B* **55** (1997) R6097.
17. Y. LI, W. KIM, Y. ZHANG, M. ROLANDI, D. WANG and H. DAI, *J. Phys. Chem. B* **105** (2001) 11424.
18. Y. ZHANG, Y. LI, W. KIM, D. WANG and H. DAI, *Appl. Phys. A* **74** (2002) 325.
19. A. LOISEAU, F. WILLAIME, N. DEMONCY and O. STEPHAN, in Proceedings of The 6th NIRIM International Symposium on Advanced Materials (ISAM'99), Tsukuba, Japan, 1999, edited by Y. Bando (National Institute for Research in Inorganic Materials) p. 45.
20. C. M. GORINGE, in Proceedings of The 6th NIRIM International Symposium on Advanced Materials (ISAM'99), Tsukuba, Japan, 1999, edited by Y. Bando (National Institute for Research in Inorganic Materials) p. 95.
21. X. BLASE, A. DE VITA, J.-C. CHARLIER and R. CAR, *Phys. Rev. Lett.* **80** (1998) 1666.

Received 16 July

and accepted 14 August 2003